



X International Conference on Structural Dynamics, EURODYN 2017

# Nonlinear vibrations of symmetric cross-ply laminates via thermomechanically coupled reduced order models

Eduardo Saetta<sup>a</sup>, Valeria Settimi<sup>a</sup>, Giuseppe Rega<sup>a\*</sup>

<sup>a</sup>*Department of Structural and Geotechnical Engineering, Sapienza University of Rome, Rome, Italy*

---

## Abstract

Thermomechanically coupled, geometrically nonlinear, laminated plates are addressed through a unified 2D formulation, by considering classical and third-order shear-deformable von Karman models, along with correspondingly consistent linear and cubic variations of the temperature along the thickness. Minimal dimension reduction of the mechanical problem is accomplished for symmetric cross-ply laminates, ending up for both models to a coupled three-mode reduced model with terms and coefficients of variable nature depending on the variety of mechanical and/or thermal excitations. Nonlinear vibrations of the classical model are investigated in conditions of thermal dynamics either passively entrained by the harmonically varying transverse load via the existing coupling terms, or also playing some active role owed to a temperature difference with respect to the surrounding medium.

© 2017 The Authors. Published by Elsevier Ltd.

Peer-review under responsibility of the organizing committee of EURODYN 2017.

*Keywords:* Laminated plates; thermomechanics; reduced order models; nonlinear vibrations; passive/active thermal dynamics; coupled response.

---

## 1. Introduction

Thermoelastic analysis of composite plates is of interest in mechanical, aerospace and civil engineering, where they may have a variety of applications. Partial or full thermomechanical coupling has been addressed in the literature mostly through finite element models, focusing on statics and linear dynamics [1], with only few studies on nonlinear dynamics [2,3]. Yet, to the latter aim, low-order models preserving the main nonlinear dynamic features of the underlying continuum formulation [4] may play a fundamental role for grasping the basic effects of the actual

---

\* Corresponding author. Tel.: +39-06-49919195; fax: +39-06-49919192.

E-mail address: [giuseppe.rega@uniroma1.it](mailto:giuseppe.rega@uniroma1.it)

coupling without introducing the complicatedness often occurring in the interpretation of nonlinear phenomena when using much richer models, also possibly implemented within an effective unified framework.

In this paper, thermomechanically coupled, geometrically nonlinear, laminated plates are addressed through a unified 2D formulation that integrates mechanical and thermal aspects. Classical and third-order shear-deformable von Karman models are considered, along with correspondingly consistent linear and cubic variations of the temperature along the thickness. Minimal dimension reduction of the mechanical problem is accomplished for symmetric cross-ply laminates, by linking both in-plane displacement components and shear-rotation angles (for the sole third-order model) to the transverse displacement and the thermal variables via kinematic condensations performed at the continuous and discretized levels, respectively. For both models, this leads to a coupled three-mode (one mechanical and two thermal) reduced model with terms and coefficients of variable nature, also depending on the variety of mechanical and/or thermal excitations. Then, focusing on the classical model, nonlinear vibrations are investigated through continuation techniques and classical tools of nonlinear dynamics (bifurcation diagrams, phase portraits, cross-sections of multidimensional basins of attraction, etc.), in conditions of thermal dynamics either passively entrained by the harmonically varying transverse load via the existing coupling terms or also playing some active role owed to a temperature difference with respect to the surrounding medium.

## 2. Continuum 2D formulation

Consider a laminated rectangular plate with mid-plane coinciding with the  $xy$  plane of an orthogonal Cartesian coordinate system, thickness  $h$ , and edge lengths  $a$  and  $b$  in the  $x$ - and  $y$ -directions, respectively. The plate is subjected to uniform in-plane stretching forces of magnitudes  $p_x$  and  $p_y$  on its edges, to distributed mechanical transverse excitation, and to thermal excitations. A unified scheme for the formulation of the relevant thermomechanical problem was presented in [5], by identifying generalized 2D variables and governing equations for both the mechanical and thermal aspects of the problem. Such a scheme virtually embeds a multitude of possible models resulting from different mechanical and thermal assumptions [6], two of which are considered here, namely the Classical (shear-indeformable) and the Third-order (shear-deformable) von Karman models with Thermomechanical Coupling, respectively labelled CTC and TTC, referring to [5] and [7] for their detailed formulations.

The 2D formulation of the two models depends on the form of the basic assumptions 3D  $\rightarrow$  2D for the configuration variables displacement and temperature (the latter to be intended as variation with respect to a reference value), which read as follows:

for the CTC model,

$$u_1 = u + zw_{,x}, \quad u_2 = v + zw_{,y}, \quad u_3 = w, \quad T = T_0 + zT_1,$$

for the TTC model,

$$u_1 = u + z\phi_1 - \frac{4}{3h^2} z^3 (\phi_1 + w_{,x}), \quad u_2 = v + z\phi_2 - \frac{4}{3h^2} z^3 (\phi_2 + w_{,y}), \quad u_3 = w, \quad T = T_0 + zT_1 + z^2T_2 + z^3T_3,$$

where  $u_i(x, y, z, t)$ ,  $i = 1, 2, 3$  are the components of the 3D displacement along the  $x$ ,  $y$  and  $z$  directions,  $u(x, y, t)$ ,  $v(x, y, t)$  and  $w(x, y, t)$  are the unknown mid-plane displacement components of the 2D model along the  $x$ ,  $y$  and  $z$  directions,  $\phi_1(x, y, t)$  and  $\phi_2(x, y, t)$  are the rotations of a transverse normal about the  $y$ - and  $x$ -axes,  $T(x, y, z, t)$  is the 3D temperature, and  $T_0(x, y, t)$ ,  $T_1(x, y, t)$ ,  $T_2(x, y, t)$ ,  $T_3(x, y, t)$  are the unknown temperature components of the 2D model.

Both CTC and TTC consider consistent variations of 3D displacement and temperature along the transverse  $z$  direction, respectively linear and cubic. It is worth noting that the greater richness of the assumed temperature variation along the thickness entails meaningful effects in terms of analysis potential of the TTC model with respect to the CTC one, though still constraining the temperature transverse shape with respect to the possibly involved variation patterns observable for non-thin laminates in some practical situations [1]. Indeed, it allows to consider a variety of thermal conditions to be possibly prescribed on the upper and lower surfaces of the laminated plate to represent variable (pure or mixed) combinations of technical interests, i.e. free heat exchange, thermal insulation, temperature prescribed, or heat flow prescribed, in contrast with the sole condition of free heat exchange to be

possibly taken into account by the CTC model, based on the assumed linear variation of the temperature field. This also enables to express the two thermal components  $T_2$  and  $T_3$  of the TTC model in terms of the membrane ( $T_0$ ) and bending ( $T_1$ ) ones, thus overall ending up to an expression of the temperature field

$$T = f_a(z) T_0 + f_b(z) T_1 + f_c(z),$$

with  $f(z)$  known functions depending on the imposed thermal boundary conditions, which is conveniently governed by only two thermal unknowns ( $T_0$  and  $T_1$ ) also in the TTC model, while keeping a richer variation along the thickness than the CTC one. Details of the procedure can be found in [7]. In contrast, at the continuum level, the mechanical unknowns are three for CTC  $\{u \ v \ w\}$  and five for TTC  $\{u \ v \ w \ \phi_1 \ \phi_2\}$ .

For each model, combining configuration, balance and phenomenological equations leads to the governing coupled partial differential equations (PDEs) of the laminated plate – which are five (three mechanical + two thermal) for CTC [5] and seven (five mechanical + two thermal) for TTC [7], respectively – along with the corresponding boundary conditions.

### 3. Minimal reduced order modeling

A dimensional reduction of the 2D continuous models is performed by expressing 2D displacement and temperature in terms of corresponding time-dependent reduced variables, through an assumed mode technique. Referring to the TTC model for its major generality, a minimal reduced order model (ROM) suitable for in-depth investigations of the nonlinear dynamics in the absence of internal resonance is obtained through the following single-mode approximation of the five 2D configuration variables  $w$ ,  $\phi_1$ ,  $\phi_2$ ,  $T_0$  and  $T_1$ ,

$$w(x, y, t) = W(t) \sin \frac{\pi x}{a} \sin \frac{\pi y}{b}, \quad \phi_1(x, y, t) = \phi_{R1}(t) \cos \frac{\pi x}{a} \sin \frac{\pi y}{b}, \quad \phi_2(x, y, t) = \phi_{R2}(t) \sin \frac{\pi x}{a} \cos \frac{\pi y}{b},$$

$$T_0(x, y, t) = T_{R0}(t) \sin \frac{\pi x}{a} \sin \frac{\pi y}{b}, \quad T_1(x, y, t) = T_{R1}(t) \sin \frac{\pi x}{a} \sin \frac{\pi y}{b},$$

in two steps involving kinematic condensations of mechanical variables performed at different levels [7,8].

(i) Under proper conditions (which include symmetric cross-ply laminates and frequencies of in-plane vibration much higher than frequencies of transverse vibration), the in-plane mechanical equations of the continuous model (considered as a linear differential system) are solved via a condensation procedure making use of solutions

$$u = f_u(W, T_{R0}), \quad v = f_v(W, T_{R0})$$

which identically satisfy the edge conditions (herein assumed movable, and subjected to uniform stretching forces), and allow us to end up to a system of only five Galerkin discretized equations (three mechanical out-of-plane + two thermal) in the five reduced variables  $W$ ,  $\phi_{R1}$ ,  $\phi_{R2}$ ,  $T_{R0}$ ,  $T_{R1}$ .

(ii) A further condensation is performed at the discretized level on the two shear-rotation angles ODEs (considered as a linear algebraic system), whose reduced unknowns  $\phi_{R1}$  and  $\phi_{R2}$  are expressed as

$$\phi_{R1} = g_{R1}(W, T_{R1}), \quad \phi_{R2} = g_{R2}(W, T_{R1}),$$

overall ending up to a system of only three discretized thermomechanically coupled nonlinear equations (one transverse mechanical + two thermal) in the three reduced time-dependent variables  $W$ ,  $T_{R0}$ ,  $T_{R1}$ . In the case of isothermal edges and free heat exchange on the upper and lower surfaces, they read in nondimensional form

$$\ddot{W} + a_{12} \dot{W} + (a_{13} + a_{14})W + a_{15}W^3 + a_{16}T_{R1} + a_{17}W \cdot T_{R0} = a_{18}F_3^{(0)} \quad (1)$$

$$\dot{T}_{R0} + a_{24}T_{R0} + a_{25}\dot{W} \cdot W + a_{26}T_{R0} = a_{27}E^{(0)} \quad (2)$$

$$\dot{T}_{R1} + a_{32}T_{R1} + a_{33}\dot{W} = a_{34}E^{(1)}, \quad (3)$$

and exhibit the same structure as that of the minimal ROM obtainable (via the sole step (i)) for the CTC model, when referring to a laminate in the same mechanical and thermal conditions. The differences between the two

ROMs only stand in the expressions of the coefficients, which in the TTC model are more involved for also incorporating the underlying shear deformability and higher order displacement and temperature assumptions.

However, with the TTC model, a greater variety of thermal boundary conditions on the external surfaces can be considered, as already mentioned. This entails obtaining again a three-dof ROM, however with possibly additional coupling terms and new thermal forcing terms present in all equations.

#### 4. Sample effects of thermomechanical coupling on the nonlinear response of CTC model

To highlight the effects of thermomechanical coupling reference is made to the CTC model, for which a comprehensive analysis of the nonlinear dynamics has been carried out by identifying the main periodic responses and their stability, and by evaluating the robustness of the basins of attraction as a function of several control parameters. In the following, response scenarios of an orthotropic single layer plate of dimensions  $a = b = 1 \text{ m}$  and  $h = 0.01 \text{ m}$  are exemplarily presented for two distinct thermal regimes, by also comparing the results with those furnished by the purely mechanical (i.e., uncoupled) model, in both the transient and steady state regimes.

**Passive thermal dynamics.** In the absence of thermal excitation ( $T_\infty = E^{(0)} = E^{(1)} = 0$ ), reference is made to an epoxy/carbon fiber composite with high thermal conductivity and low specific heat, specifically designed to activate thermal processes with no computational criticalities, while also achieving a transverse strength of the plate such to entail physically admissible displacements. The relevant physical properties are:  $Y_1=6.39 \cdot 10^{11} \text{ N/m}^2$ ,  $\nu_{12}=0.31$ ,  $\rho=2003.6 \text{ kg/m}^3$ ,  $\lambda_{11}=2520.1 \text{ W/(m}\cdot\text{K)}$ ,  $\alpha_1=1.47 \cdot 10^{-5} \text{ 1/K}$ ,  $c_v=244 \text{ J/(kg}\cdot\text{K)}$ ,  $Y_2=6.21 \cdot 10^9 \text{ N/m}^2$ ,  $G_{12}=2.23 \cdot 10^9 \text{ N/m}^2$ ,  $\lambda_{22}=3.18 \text{ W/(m}\cdot\text{K)}$ ,  $\alpha_2=-1.91 \cdot 10^{-6} \text{ 1/K}$ ,  $\delta=330 \text{ (N}\cdot\text{s)/m}^3$ ,  $H=100 \text{ W/(m}^2\cdot\text{K)}$ , where 1 and 2 subscripts refer to properties in  $x$  and  $y$  direction, respectively, and the physical meaning of the various parameters is that described in [5]. The numerical investigations developed as a function of the most significant mechanical parameters (i.e. forcing amplitude of the harmonic mechanical excitation  $F_3^{(0)}$  at primary resonance, pretension) show a minor effect of the thermomechanical coupling, that consists of the mere activation of the thermal variables, which are dragged by the mechanics and which stabilize around a slightly shifted equilibrium with respect to the trivial position. Yet, analyzing the dynamical effects of intrinsic thermal parameters may allow to identify those possibly affecting the nonlinear response in such a way to be properly taken into account in the design stage for securing the wanted behavior. Among them, the thermal expansion  $\alpha_2$  of the material, which of course is not included in the purely mechanical model, is seen to have a substantial role in modifying the system dynamics, as shown in Fig. 1. There, the bifurcation diagrams with increasing  $\alpha_2$  are presented, for  $f=1$ ,  $\eta=1$ , representing amplitude and frequency of the mechanical excitation, and  $p=4$ , which governs the  $a_{14}$  coefficient of Eq. (1) ( $a_{14}=p/\eta$ ) and corresponds to a pretension much higher than the linear buckling value, thus implying the presence of buckled configurations. For the  $\alpha_2$  value of the reference material ( $\alpha_2=-1.91 \cdot 10^{-6} \text{ (1/K)}$ ), the response scenario is characterized by two couples of stable 1-period buckled solutions which coexist with a 1-period cross-well response and two 4-period solutions. Increasing the thermal expansion causes a reduction of the multistability which disappears at  $\alpha_2=6.95 \cdot 10^{-3}$ , where the only stable solution is the pair of low-amplitude buckled responses. Such local behavior is confirmed by the evolution of the basins of attraction of the 4D model (see Eqs. (1)-(3)) for increasing  $\alpha_2$ , as shown by the relevant cross-sections in the  $(W, \dot{W})$  plane with  $T_{R0}(0) = T_{R1}(0) = 0.0$ , reported in Fig. 1(b). The marked fractality which affects all basins for the reference  $\alpha_2$  value is strongly reduced as the thermal expansion increases, and the phase portrait becomes more and more regularly organized, with a clear separation of the initial conditions leading to the various attractors. Finally, for  $\alpha_2 > 6.95 \cdot 10^{-3}$ , the sign of the initial displacement determines the buckled response to be achieved.

**Active thermal dynamics.** When thermal sources are directly applied, other remarkable results come into play. The relevant analysis has been conducted considering a different kind of material [1], whose higher values of the  $a_{24}$  and  $a_{26}$  coefficients with respect to the previous one allow to unveil meaningful system dynamics by applying thermal excitations with practically acceptable values. The relevant physical properties are:  $Y_1=1.72 \cdot 10^{11} \text{ N/m}^2$ ,  $\nu_{12}=0.25$ ,  $\rho=1940 \text{ kg/m}^3$ ,  $\lambda_{11}=36.42 \text{ W/(m}\cdot\text{K)}$ ,  $\alpha_1=0.57 \cdot 10^{-6} \text{ 1/K}$ ,  $c_v=400 \text{ J/(kg}\cdot\text{K)}$ ,  $Y_2=6.91 \cdot 10^9 \text{ N/m}^2$ ,  $G_{12}=3.45 \cdot 10^9 \text{ N/m}^2$ ,  $\lambda_{22}=0.96 \text{ W/(m}\cdot\text{K)}$ ,  $\alpha_2=35.6 \cdot 10^{-6} \text{ 1/K}$ ,  $\delta=330 \text{ (N}\cdot\text{s)/m}^3$ ,  $H=100 \text{ W/(m}^2\cdot\text{K)}$ . The effect of a thermal excitation is evaluated by considering the plate in a high temperature environment (i.e.  $T_\infty \neq 0$  in Eq. (2)). The direct activation of the membrane thermal variable  $T_{R0}$  contributes to system pretension via a parametrically varying increase of the linear mechanical stiffness, which is responsible for triggering buckling.

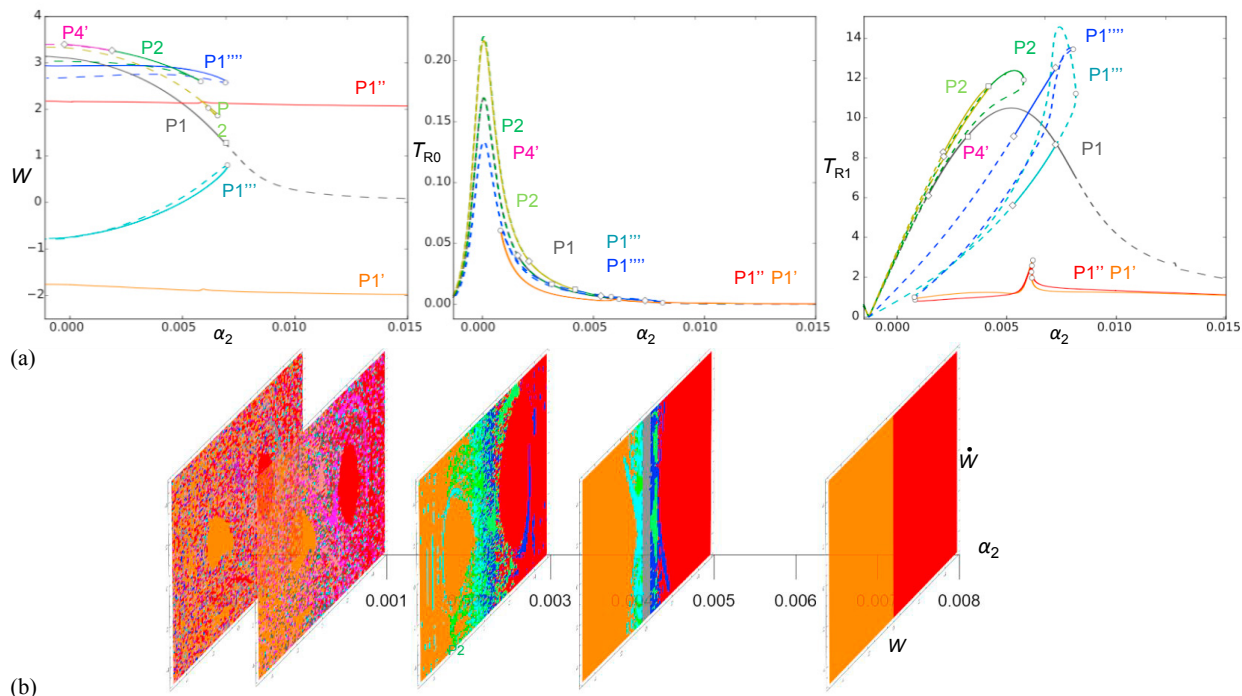


Fig. 1. Bifurcation diagrams of displacement, membrane, and bending temperatures with varying thermal expansion  $\alpha_2$ , for  $f = 1, \eta = 1, p = 4$ , with saddle-node (circle), transcritical (square), period-doubling (diamond) bifurcations (a). Basins of attraction in the  $(W, \dot{W})$  plane, for  $T_{R0}(0)=T_{R1}(0)=0.0$ , at  $\alpha_2 = -1.91 \cdot 10^{-6}, \alpha_2 = 1.0 \cdot 10^{-3}, \alpha_2 = 3.0 \cdot 10^{-3}, \alpha_2 = 5.0 \cdot 10^{-3}, \alpha_2 = 8.0 \cdot 10^{-3}$ , with colors corresponding to periodic solutions (b).

Thus, the displacement bifurcation diagram in Fig. 2(a) can be obtained by varying either the mechanical pretension  $p$ , as also furnished by the uncoupled mechanical model, or the thermal excitation  $T_\infty$ . With a mechanical pretension ( $p = 2.51$ ) slightly lower than the value giving rise to buckled 1-period solutions, a monostable cross-well dynamical configuration occurs, as also shown by the cross-section of the 4D basins of attraction for  $T_{R0}(0) = T_{R1}(0) = 0.0$  (Fig. 2(b)). When adding a thermal excitation  $T_\infty = 100$ , Fig. 2(a) reveals that the system response is characterized by a multistable behavior including a pair of buckled solutions, in addition to the pre-buckling cross-well response. Yet, the cross-section of the 4D basins of attraction with trivial thermal variables still displays the monostable scenario of Fig. 2(b). The discrepancy between expected and actual behaviors can be understood by looking at the time histories in Fig. 2(d). The long transient time needed by the membrane temperature to attain its final steady value (mid-subfigure) entails, in the mechanical equation, a slowing of the thermal contribution to the mechanical stiffness which is necessary to achieve the buckled configuration. As a consequence, the mechanical response quickly falls back onto the pre-buckling solution, which remains stable also after the arise of the steady buckled responses, thus representing a robust attractor for the system in the whole range of considered parameters.

Conversely, the buckled configuration is caught at once by the global response (Fig. 2(c)) of the uncoupled mechanical system with constant thermal distortion  $T_{R0} = 0.9$ , i.e. the steady value attained by the membrane thermal variable in its temporal evolution (Fig. 2(d)). The same phase portrait would indeed be obtained with the fully coupled model by looking at the cross section of the 4D basin of attraction at steady values of the two thermal variables, where all the pre- and post-buckling attractors are located. However, the wrong global information provided by the uncoupled mechanical oscillator as to the buckled outcome of a huge amount of  $(W, \dot{W})$  initial conditions actually ending up to the pre-buckled solution clearly highlights the need to consider the actual thermomechanically coupled model in the nonlinear dynamic analysis or, in different words, the care to be paid in using tools as the basins of attraction, suitable to describe steady responses, for the analysis of processes, like the thermal one, also involving meaningful transients.

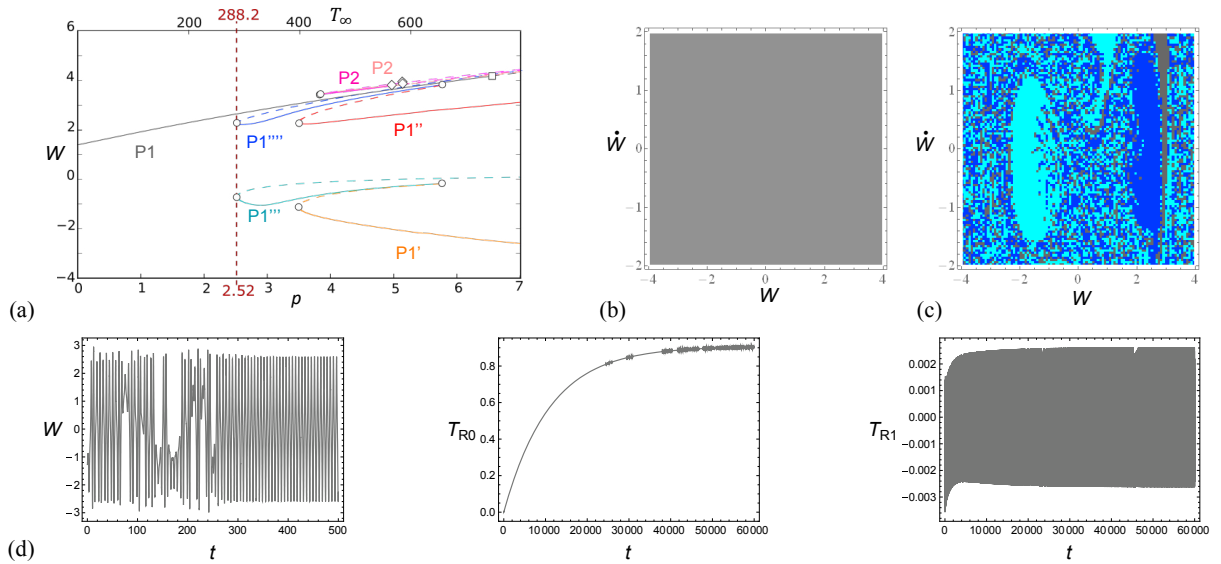


Fig. 2. Bifurcation diagram as a function of pretension  $p$  and thermal variation  $T_\infty$ , for  $f=1$ ,  $\eta=1$ , with saddle-node (circle), transcritical (square), and period-doubling (diamond) bifurcations (a). Basins of attraction in the  $(W, \dot{W})$  plane for  $p = 2.51$ : of the thermomechanical model, for  $T_{R0}(0) = T_{R1}(0) = 0.0$ , also when adding  $T_\infty = 100$  (b), of the uncoupled mechanical system, with  $T_{R0} = 0.9$  (c). Time histories of the former model (d).

## 5. Concluding remarks

Basic aspects of two thermomechanically coupled models of laminated plates with different richness have been provided at both continuum and discretized levels. The simpler model has been then used to highlight sample effects of thermomechanical coupling on the nonlinear response in conditions of either passive or active thermal dynamics. In absence of thermal excitations the important role played by some physical properties of the material in strongly modifying the system response has been pointed out, while the addition of thermal changes underlines the critical effect of the transient coupled thermal dynamics on also the mechanical steady behavior.

## Acknowledgements

The authors acknowledge the financial support of PRIN 2015 “Advanced mechanical modeling of new materials and structures for the solution of 2020 Horizon challenges” (No. 2015JW9NJT).

## References

- [1] S. Brischetto, E. Carrera, Thermomechanical effect in vibration analysis of one-layered and two-layered plates, *International Journal of Applied Mechanics*. 3(1) (2011) 161-185.
- [2] P. Ribeiro, Thermally induced transitions to chaos in plate vibrations, *Journal of Sound and Vibration*. 299 (2007) 314–330.
- [3] F. Alijani, Bakhtiari-Nejad, M. Amabili, Nonlinear vibrations of FGM rectangular plates in thermal environments, *Nonlinear Dynamics*. 66(3) (2011) 251-270.
- [4] Y.L. Yeh, The effect of thermo-mechanical coupling for a simply supported orthotropic rectangular plate on non-linear dynamics, *Thin Walled Structures*. 43 (2005) 1277–1295.
- [5] E. Saetta, G. Rega, Unified 2D continuous and reduced order modeling of thermomechanically coupled laminated plate for nonlinear vibrations, *Meccanica*. 49 (2014) 1723-1749.
- [6] E. Saetta, G. Rega, Modeling, dimension reduction, and nonlinear vibrations of thermomechanically coupled laminated plates, *Procedia Engineering*. 144 (2016) 875-882.
- [7] E. Saetta, G. Rega, Third-order thermomechanically coupled laminated plates: 2D nonlinear modeling, minimal reduction, and transient/post-buckled dynamics under different thermal excitations, *Composite Structures*. (2017) doi: 10.1016/j.compstruct.2017.03.048.
- [8] G. Rega, E. Saetta, Shear deformable composite plates with nonlinear curvatures: modeling and nonlinear vibrations of symmetric laminates, *Archive of Applied Mechanics*. 82 (2012) 1627–1652.